Applied Energy 280 (2020) 115987

Contents lists available at ScienceDirect

Applied Energy

journal homepage: www.elsevier.com/locate/apenergy

Triple-mode grid-balancing plants via biomass gasification and reversible solid-oxide cell stack: Concept and thermodynamic performance

Ligang Wang [a,*], Yumeng Zhang [a], Chengzhou Li [a], Mar Pérez-Fortes [b], Tzu-En Lin [c], François Maréchal [d], Jan Van herle [b], Yongping Yang [a]

[a] Innovation Research Institute of Energy and Power, North China Electric Power University, China
[b] Group of Energy Materials, Swiss Federal Institute of Technology in Lausanne, Switzerland
[c] Institute of Biomedical Engineering, National Chiao Tung University, Taiwan, Republic of China
[d] Industrial Process and Energy Systems Engineering, Swiss Federal Institute of Technology in Lausanne, Switzerland

ARTICLE INFO

Keywords:
Waste-to-energy
Grid balancing
Gasification
Power-to-x
Reversible solid-oxide cell
Sector coupling

ABSTRACT

Biomass-to-electricity or -chemical via power-to-x can be potential flexibility means for future electrical grid with high penetration of variable renewable power. However, biomass-to-electricity will not be dispatched frequently and becomes less economically-beneficial due to low annual operating hours. This issue can be addressed by integrating biomass-to-electricity and -chemical via "reversible" solid-oxide cell stacks to form a triple-mode grid-balancing plant, which could flexibly switch among power generation, power storage and power neutral (with chemical production) modes. This paper investigates the optimal designs of such a plant concept with a multi-time heat and mass integration platform considering different technology combinations and multiple objective functions to obtain a variety of design alternatives. The results show that increasing plant efficiencies will increase the total cell area needed for a given biomass feed. The efficiency difference among different technology combinations with the same gasifier type is less than 5% points. The efficiency reaches up to 50%–60% for power generation mode, 72%–76% for power storage mode and 47%–55% for power neutral mode. When penalizing the syngas not converted in the stacks, the optimal plant designs interact with the electrical and gas grids in a limited range. Steam turbine network can recover 0.21–0.24 kW electricity per kW dry biomass energy (lower heating value), corresponding to an efficiency enhancement of up to 20% points. The difference in the amounts of heat transferred in different modes challenges the design of a common heat exchange network.

1. Introduction

Biomass is referred to as the biodegradable fraction of (i) products, (ii) waste and residues from a biological origin, from agriculture, forestry and related industries, as well as (iii) industrial and municipal wastes [1]. In 2017, biofuels accounted for 56% of the primary renewables production in EU-28 (225 Mtoe), with solid, gas, liquid forms contributing 42%, 7.4% and 6.7%, respectively [2]. Biomass is dominating and will continue to provide the bulk of renewables for heating/cooling and transport sectors in the next decades [3]. The electricity generated from biomass is also increasing; however, its share in the renewable-derived electricity remains at 11%–12% since 2005 [4].

In the electricity sector, the fast-growing intermittent renewable power asks for increased grid flexibility, which is expected to be covered by various flexibility means in Europe, including grid interconnection, controllable renewable power, thermal power plants, demand-side management, and energy storage [5]. However, when the penetration of intermittent renewable power becomes high enough that energy is no longer a limiting factor, thermal power plants with high operating costs will not be dispatched frequently and become even more unprofitable due to low annual operating hours [3]. This situation will be faced by biomass power plants due to the operating costs related to the biomass supply chain. Thus, there is a strong need for innovative biomass utilization for future energy-system scenarios.

Biomass can be an effective, low carbon alternative for power storage and grid balancing. This could be achieved by gasification based biomass-to-chemicals enhanced by power-to-x capability. By injecting renewable-derived hydrogen into gasification-derived syngas to adapt its composition, the expensive, energy-intensive carbon capture unit equipped in conventional biomass-to-chemicals can be avoided. Particularly, high-temperature power-to-x via solid-oxide electrolyzer (SOE)

* Corresponding author.
E-mail address: ligang.wang@ncepu.edu.cn (L. Wang).

https://doi.org/10.1016/j.apenergy.2020.115987
Received 3 July 2020; Received in revised form 1 October 2020; Accepted 3 October 2020
Available online 8 October 2020

Nomenclature

Abbreviations

ASU	Air separation unit
CAPEX	Capital expenditure
CC	Cold gas cleaning
CE	Co-electrolysis
EFG	Entrained-flow gasifier
EL	Electrolyzer
FC	Fuel cell
FICFB	Fast internally circulating fluidized-bed
HC	Hot gas cleaning
HEN	Heat exchanger network
HTS	High-temperature stage
LHV	Lower heating value
MILP	Mixed-integer linear programming
PowGen	Power generation
PowNeu	Power neutral
PowSto	Power storage
PYR	Pyrolysis
QC	Quenching
RP	Radiant panel
RSOC	Reversible solid-oxide cell
SE	Steam electrolysis
SNG	Synthesis natural gas
SOE	Solid-oxide electrolyzer
STN	Steam turbine network
TAR	Tar reformer
TOR	Torrefraction

Mathematical Symbols

$\dot{E}$	Energy flow
η	Energy efficiency
C	Cost

Subscripts

bio	Biomass
db	Dry basis
ele	Electricity

is preferred due to its high efficiency and process-integration capability. Thus, in our previous studies [6–8], SOE integrated biomass-to-synthesis natural gas (SNG), -methanol, -dimethyl ether, -jet fuel and -ammonia have been intensively evaluated in a techno-economical manner. It is concluded that the overall efficiency of biomass-to-chemical can be significantly enhanced by 5%–17% points; however, the economic performance depends strongly on the availability of excess renewable power [9], since a low availability needs an oversized power-to-x or to equip both power-to-x and carbon capture unit [7].

A dual-mode grid-balancing plant enabled by reversible solid-oxide cell (RSOC) stack can shift between power generation (PowGen) and power storage (PowSto), thus providing grid services of both up- and down-regulation with high annual operating hours. Several researchers have investigated the thermodynamic performances of different system concepts with the round-trip efficiency reaching over 70% for large-scale electricity storage combining RSOC with underground storage of CO_2 and CH_4 [10], 54%–60% when combining RSOC with thermal storage [11,12], and 60% when integrating RSOC system with natural gas and carbon capture infrastructures [13]. The scheduling of the two modes depends on the applications and may require additional CO_2 sources. This could be solved by combining biomass with RSOC systems, which can convert biomass into electricity during power shortage or to chemicals during power surplus. In literature, only few case studies of such a concept were found, e.g., (1) a two-stage gasifier fueled by wood chips [14] with a recent update in Ref. [15], where four operating modes are proposed to cope with different electricity prices, and (2) a plasma gasifier fueled by municipal solid wastes [16]. Unfortunately, the performances reported there are limited to the level of case study and are even not comparable with each other due to different efficiency definitions.

The flexibility of the dual-mode grid-balancing plant can be further enhanced by a power neutral (PowNeu) mode, under which the plant produces chemicals with the electricity generated internally and thus the plant can be isolated from the electrical grid as capacity reserves. In this case, we propose a triple-mode (PowGen, PowSto and PowNeu) grid balancing plant concept based on biomass gasification and RSOC. Such a concept allows for (1) enhanced annual full-load operating hours (nonstop operation over the year if no maintenance needed), (2) reduced investment by sharing hardware (particularly, the stacks) among three modes and avoiding carbon capture unit, (3) additional profits from providing grid-balancing services in forms of both energy balancing and capacity reserves, and (4) enhanced storage capability and capacity. Particularly, when SNG is targeted to produce and can be injected into the gas grid, the storage capacity will not be a limiting factor with the existing, large-scale gas infrastructure (over 1100 TWh in Europe) [17].

The deployment of such triple-mode grid-balancing plants is constrained by the plant design, grid imbalance to be handled and biomass supply chain, thus restricted to a specific geographical area. These factors should be considered systematically and simultaneously to find realistic business cases. To cope with this complex optimization problem, the generic decomposition-based methodology for optimal deploying dual-mode RSOC systems proposed by the authors in Ref. [18] is modified in this paper to further consider biomass supply chain.

Therefore, the innovation of the paper is the modified business-case identification method including the optimal conceptual design of such novel biomass-based multi-mode plants. The major task of this paper is to establish a database of optimal trade-off plant designs considering (1) various process options, (2) optimal heat cascade utilization, (3) optimal placement and sizing of steam turbine network (STN) to recover process waste heat, and (4) multiple objective functions. Based on the design database obtained, the overall methodology will be implemented in the follow-up papers to find promising business cases in Denmark and South Italy for 2030, where variable renewable energy sources are expected to be dominating.

The remaining paper is organized as follows: In Section 2, the concept of the triple-mode plant is introduced with system boundaries and process options. Then, the overall methodology is described in Section 3 with detailed specifications and considerations for optimal plant conceptual design. In Section 4, the trade-off designs for different process options are discussed by emphasizing the heat utilization of different modes and the importance of the STN. Finally, conclusions are drawn in Section 5.

2. Concept of the triple-mode grid-balancing plant

2.1. Concept

The generic concept of the triple-mode plant is illustrated in Fig. 1, with the processes of biomass-to-gas via gasification or fermentation, and gas-to-product. Biomass-to-syngas is considered in this paper and is expected to operate without load shifting, while the clean syngas produced is converted in three modes, thanks to the coordination of two RSOC blocks:

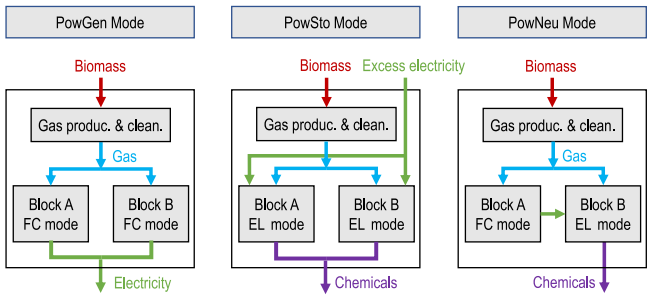

Fig. 1. The generic concept of the triple-mode grid-balancing plant.

(1) PowGen mode: biomass-to-electricity with both RSOC blocks under the fuel cell (FC) mode.

(2) PowSto mode: biomass-to-chemical with both RSOC blocks under the electrolyzer (EL) mode to enable the power-to-x capability powered by excess renewable electricity.

(3) PowNeu mode: biomass-to-chemical with one RSOC block under the FC mode to power the other block under the EL mode for chemical production. No external electricity is needed.

2.2. System boundary

The overall system and the system considered here are illustrated in Fig. 2. This paper focuses on the energy conversion of the plant itself, thus does not consider biomass collection and the interaction with the electrical grid. The oxygen as the gasification agent is managed with buffer tanks, charged by the RSOC blocks under EL mode and a standalone air separation unit (ASU, if needed), and discharged to the market when excess. However, the ASU itself is not considered in this paper, since its sizing depends on the plant scheduling determined by specific applications. The waste heat utilization, e.g., for district heating, depends highly on local circumstances and thus is not included in the efficiency definition. The final chemical product is assumed to be SNG, which is injected into the gas transmission network. Therefore, the key system boundaries are:

(1) Biomass: For agricultural residues and forest wood, since the lower heating value on a dry basis (LHVdb) usually varies within 18–20 MJ/kg [19], the properties considered are C 50.81 wt.%, H 5.96 wt.%, O 43.05 wt.%, N 0.18 wt.% with the LHVdb being 19.1 MJ/kg, and a humidity of 0.5 kg-H_2O/kg-biomass. For the wastes, represented by municipal solid waste, the approximate analysis considered is moisture 20%, fixed carbon 10.23%, volatile matter 75.90% and ash 13.81%, resulting in a LHVdb of 19.4 MJ/kg [16].

(2) Oxygen storage conditions: 200 bar and 30 °C.

(3) Grid injection: 80 bar, methane molar fraction > 96%. The variation of injection pressure has a negligible impact on the plant's performances.

2.3. Process options

There are many technology options available for pretreatment, gasification, syngas cleaning and conditioning, and syngas-to-SNG, e.g., Fig. 3 considered for this paper. Considering the sizes of the gasifiers, two types of gasifiers are involved in this paper: (1) entrained-flow gasifier with direct heating (EFG, 1200–1500 °C, 30–80 bar) for large-scale applications (100–1000 MWth), (2) twin (dual) fluidized-bed gasifier, e.g., fast internally circulating fluidized-bed (FICFB, 800–1000 °C, 1–4 bar) for medium-scale applications (10–100 MWth). Plasma gasifier (4000 °C, 1 bar) for small-scale applications (1–30 MWth) are not considered. The biomass pretreatment considers air drying and torrefaction (only for EFG). Syngas cooling can be done by water/steam quenching (QC) or radiant panel (RP) for steam generation. Tar removal is needed mainly for FICFB due to a low gasification temperature and it can be done by a high-temperature stage (HTS) up to 1300 °C or catalytic tar reforming (TAR). The syngas-to-SNG can be achieved by two means: (1) steam electrolysis with the produced hydrogen injected to syngas for methanation, and (2) co-electrolysis of H_2O and CO_2 with syngas directly sent into the stack to adjust the composition for methanation. These technologies have been described in detail in the supplementary materials.

3. Methodology of optimal deployment

3.1. Overall methodology for business case identification

The overall target is to identify promising future business cases for such grid-balancing plants from a set of well-defined case studies. A case study must seat on a specific geographical zone to consider realistic (or reasonably predicted) grid-flexibility needs and biomass availability. However, in one single optimization problem, it is difficult to simultaneously consider the nonlinear programming for optimal conceptual plant design and the mixed-integer programming for optimal plant scheduling to cope with a specific imbalance profile [18], not even to mention the computation-expensive supply chain optimization. Thus, it is necessary to decompose the overall complex optimization problem for high solvability. Although global optimum is not guaranteed, it is believed that the optimal solutions obtained are good enough for practical applications.

We propose a decomposition based, sequential approach (Fig. 4), summarized as follows:

(1) *Identification of (future) grid flexibility needs*. Based on the multi-timescale data-driven method presented in Ref. [20], for the zone considered, hourly timeseries of the fluctuating discrepancies between variable renewable energy production and electricity consumption are generated for step (4).

(2) *Identification of (future) biomass availability*. In compliance with the classification schemes and methodology applied in the projects like BEE [21], S2Biom [22] and BIOMASS FUTURE [23], the biomass streams in the zones interested are assessed with further available Directives, Regulations and Reports, to build the geodatabase with their weight, characteristics and location coordinates for step (5).

(3) *Optimization of conceptual plant design*. As extensively discussed in our previous papers [18,24–26], the design points of the components, particularly the stacks, strongly affect the thermodynamic performances of the plant and further the economics of the overall application. Therefore, instead of one single design, a pool of trade-off designs is generated for each process option and fed to step (4).

(4) *Optimization of design selection, plant sizing and scheduling to satisfy the flexibility needs*. With hourly flexibility needs from step (1) and multiple plant designs from step (3), the Dispa-SET platform [27] has been modified to determine the number, design, size and scheduling of the plants employed to maximize the gain from grid-balancing services and the sale of SNG by subtracting the costs of auxiliaries to assist the continuous operation of all plants, e.g., oxygen tanks, ASU. Note that the capital expenditures (CAPEXs) of the plants are not considered at this step. The input biomass energy needed for each plant is provided to step (5), while the gain is fed to step (6).

(5) *Optimization of the biomass supply chain*. With the biomass geodatabase from step (2) and the biomass energy needed for each plant from step (4), the costs of biomass supply chain and pretreatment are minimized with the superstructure-based method presented in Refs. [28–30] and fed to step (6).

(6) *Identification of target capital expenditure*. The target CAPEX of the grid-balancing plants employed can be further calculated based on the gain from step (4) and the costs related to biomass collection from step (5).

(7) *Identification of the feasibility of the case study*. With the plant details from step (4), the CAPEX of each plant is evaluated at different conditions, e.g., different specific investment costs of the stack, to determine the prerequisites for potential business cases.

The work presented here focuses on the red-colored task in Fig. 4 to generate a pool of trade-off design alternatives.

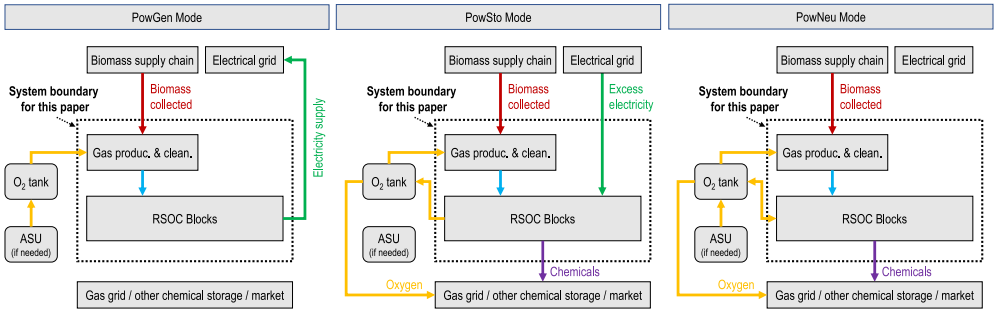

Fig. 2. The overall system and system boundary considered in this paper.

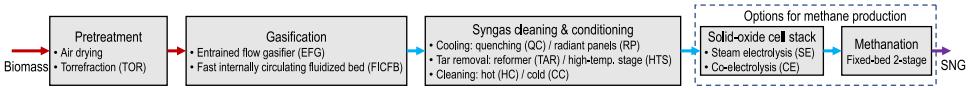

Fig. 3. Process options considered in this paper with the stack section showing only the options for methane production.

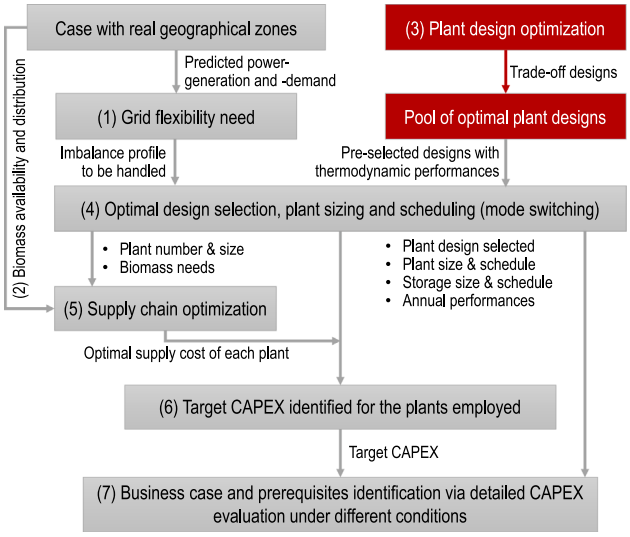

Fig. 4. The overall decomposition-based methodology to identify feasible business cases for the grid-balancing plants. The red-colored session is handled in this paper, while the overall method will be implemented in the follow-up papers.

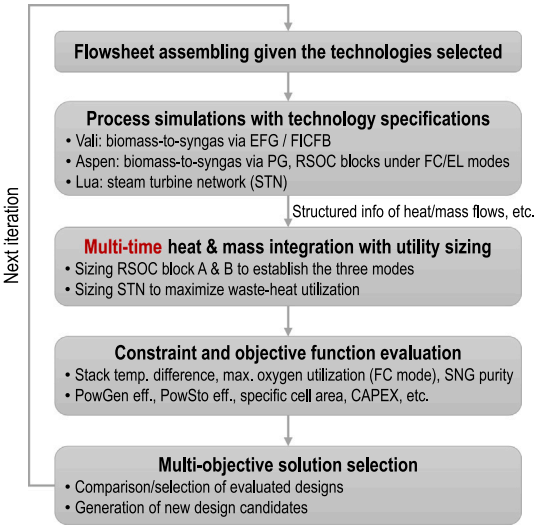

Fig. 5. The method for optimal conceptual plant design.

3.2. Method of optimal conceptual plant design

The conceptual plant design can quickly evaluate the overall thermodynamic performances without considering a detailed design of the heat exchanger network (HEN). Our platform, recently updated as described in Ref. [31], has been applied to establish the plant design database for dual-mode RSOC based plant in Ref. [18]. The platform is further configured for the three-mode grid-balancing plant with the performance estimation and component sizing based on separate simulations of the three modes.

The iterative procedure (Fig. 5) first assembles the flowsheets of the three modes based on the specified process option, which are then simulated by professional simulators (e.g., Vali, Aspen Plus) or other means with specific technological specifications (decision variables). The resulting energy and mass flows of all three modes are formatted as the input for multi-time heat and mass integration with utility selection and sizing, formulated as a mixed-integer linear programming (MILP) problem as described in detail in Ref. [31]. The solving of this MILP problem concludes utility sizes, hot-cold and grand composite tables/curves for illustrating the heat cascade utilization, based on which the HEN area and costs can be further estimated. Practical constraints, key performance indicators and objective functions are then evaluated *a posteriori* with the access to all data from the above steps. Queuing multi-objective optimizer as a master program controls the iteration and concludes a set of Pareto plant designs.

Each mode of the plant corresponds to a time step in the multi-time MILP formulation, which sizes the two RSOC blocks (Section 2) simply via the electricity balance in the PowNeu mode (no electricity import and export). If STN is employed to recover waste heat to electricity, the ratio of the stack number in the FC/EL blocks will decrease. It is also assumed that the operating points of the FC blocks in the PowGen and PowNeu modes remain the same, so do those of the EL blocks in the PowSto and PowNeu modes. Thus, the total stack number becomes identical for all three modes.

3.3. Practical constraints and key performance indicators

The constraints evaluated posteriorly are mainly related to the stack operation, including maximum temperature difference between the stack inlet and outlet, maximum oxygen utilization, carbon deposition (evaluated via cantera [32]), etc. The effect of operating point of the stack on its lifetime can hardly be included for the scope of the paper. The grid injection of SNG is only constrained here by the purity (96 vol.%) but not the Wobbe index.

The key performance indicators involve the energy efficiencies (based on LHV) of the three modes and the investment costs of the plant:

(1) PowGen efficiency:

$$\eta_{\text{PowGen}} = \frac{\dot{E}_{\text{ele,out}}}{\dot{E}^{\text{lhv}}_{\text{bio,in}}} \tag{1}$$

(2) PowSto efficiency:

$$\eta_{\text{PowSto}} = \frac{\dot{E}^{\text{lhv}}_{\text{sng,out}}}{\dot{E}^{\text{lhv}}_{\text{bio,in}} + \dot{E}_{\text{elec,in}}} \tag{2}$$

(3) PowNeu efficiency:

$$\eta_{\text{PowNeu}} = \frac{\dot{E}^{\text{lhv}}_{\text{sng,out}}}{\dot{E}^{\text{lhv}}_{\text{bio,in}}} \tag{3}$$

(4) Specific cell area needed (m^2/kW-LHVdb):

$$\bar{A} = A_{\text{tot}} / \dot{E}^{\text{lhv}}_{\text{bio,in}} + M\, \dot{m}_{\text{syngas,burnt}} \tag{4}$$

In the above formulations, $\dot{E}$ represents the incoming (in) or outgoing (out) energy flow of biomass (bio), synthesis natural gas (sng), or electricity (elec) in the energy balance of a specific mode. The energy flows carried by materials are based on the lower heating value (lhv). The specific cell area needed ($\bar{A}$) is evaluated with a penalty term ($M\, \dot{m}_{\text{syngas,burnt}}$ with M being a big number) to suppress the syngas burnt for process heating, thus the minimization of this specific cell area can promote the amount of syngas converted by the RSOC stacks. All indicators are calculated following the procedure described in Fig. 5.

3.4. Models and specifications

Equilibrium-based steady-state models are employed. The biomass-to-syngas processes via EFG and FICFB and related technological options refers to Ref. [19]. The RSOC models for electrode-supported planar cell stack have been described for both FC and EL modes in Refs. [18,24,26] but no external reformer is needed for this paper. The isothermal 2-stage methanation system employed has been developed in Refs. [18,24]. The heat cascade utilization has been formulated in detail in Ref. [31] with the HEN area and costs estimated by the vertical heat transfer described in Ref. [33], while the STN formulation has been given in Refs. [34,35] and a 4-pressure level STN is employed with the pressures and superheating degree optimized for maximal heat recovery. The hot utilities considered is only syngas combustor, the use of which penalizes the efficiencies. More information on the models and specifications can be found in the supplementary materials.

3.5. Objective functions and decision variables

The objective functions considered are the PowGen efficiency, the PowSto efficiency and the specific cell area needed. The PowNeu efficiency is not set as an objective, since (1) it is positively related to PowGen and PowSto efficiencies, and (2) the PowNeu mode is not expected to dominate the service provided for grid balancing.

The decision variables are listed in Table 1 with other relevant specifications. Based on practical stack operation experiences, the oxygen inlet flow rate is limited to 50 sccm/cm^2 (standard cubic centimeter per minute per square centimeter) for the EL mode and 80 sccm/cm^2 for the FC mode.

4. Results and discussion

The optimal conceptual plant design is performed for the EFG and FICFB process options, respectively. An overview of the results of different process options is given first. Considering the similarity of the results, the process option EFG-TOR-HC-SE-STN is investigated in detail.

4.1. Overview

The trade-off between the efficiency and specific cell area needed to process 1 kW-LHVdb biomass is illustrated in Fig. 6 for the plant designs in the design pool obtained. Each cluster represents a set of optimal design points for a specific process option, which differ from the design variables (Table 1). The key qualitative observations are: (1) There is no big difference in the three efficiencies (less than 5% points) among different process options of the same gasifier type, e.g., EFG-TOR-HC-SE-STN, EFG-TOR-CC-SE-STN and EFG-TOR-CC-CE-STN. This is indicated by the gap between the clusters shown in Fig. 6. The selection of gas cleaning and conditioning processes has limited effect on the plant performance. This is mainly due to the overall exothermic biomass-to-syngas process and maximal recovery of process heat with STN. Particularly, the advantage of CE on heat integration, which fundamentally needs less electrical heating owing to less steam requirement as described previously in Ref. [9], becomes not effective for efficiency improvement. (2) From the design viewpoint, the increase in efficiency results in an increased cell area to process the same amount of biomass, thus an increase in the investment costs. This is mainly due to the decrease in current density needed to enhance the system efficiency.

Quantitatively, by varying the stack and STN design variables, the EFG process options (represented by EFG-TOR-HC-SE-STN, EFG-TOR-CC-SE-STN and EFG-TOR-CC-CE-STN) with STN achieve efficiencies of 42%–50% (PowGen), 62%–72% (PowSto) and 37%–47% (PowNeu). The FICFB process options with STN, represented by FICFB-HTS-RADP-HC-SE-STN, FICFB-TRF-CC-SE-STN and FICFB-TRF-CC-CE-STN, realize higher efficiencies of 42%–60% (PowGen), 54%–76% (PowSto) and 35%–55% (PowNeu). The efficiency ranges of the EFG process options are narrower than those of the FICFB.

The PowSto efficiency is higher than the PowGen efficiency, due to the efficient power-to-x, efficiency definition and STN; while the PowNeu efficiency is lower than the PowSto efficiency, since the SNG production of the PowSto mode is much (over 3 times, shown in Section 4.2.1) higher than the PowNeu mode with a large share of syngas converted to electricity to drive the electrolysis stacks. The difference in efficiency among EFG and FICFB process options is caused by the performances of stacks and STN. The stack performance is affected largely by the syngas composition, particularly the ratio $(H_2/CO_2)_{eq}$: 1.6 (FICFB) and 1.2 (EFG) for the types of biomass considered. The higher efficiency achieved by the FICFB process options is mainly due to the high $(H_2/CO_2)_{eq}$ ratio, yielding better FC performance for power generation and requiring fewer EL stacks to process the same amount of dry syngas.

The STN plays an important role to enhance the efficiencies of all three modes by heat recovery (Fig. 6). All clusters of the designs without STN (the symbols with transparency) shift towards decreased efficiency, compared with the clusters with STN. The lower the efficiencies, the more heat can be potentially recovered; thus, for the EFG and FICFB process options, the STN can contribute to an increase in the PowGen and PowSto efficiencies of up to 20% points. For all process options, the PowSto efficiency is less sensitive (up to 10% points) to the STN due to the mathematical nature of the efficiency definition (Eq. (2)): At the denominator, the constant term of biomass energy input is much larger than the net power import. The STN can recover excess heat to electricity up to 0.24 kW/kW-LHVdb for the FICFB and EFG options.

The specific cell area, the decisive factor of the investment costs, is within 0.1–0.2 m^2/kW-LHVdb biomass. An increased efficiency tends to require more cell area to process the same amount of biomass. The investment costs of the designs in the design pool can be readily evaluated based on classical cost evaluation method, e.g., Ref. [33], for different plant sizes, derived from the step (4) of the overall method described in Fig. 4.

Table 1
Decision variables or specifications.

Component	Variables or parameters	Lower bound	Upper bound	Fixed value
Stack-common	Pressure, bar			1.2
	Inlet temperature, °C			680
	Outlet temperature[a], °C	650	820	
	Single-pass reactant utilization factor, %	50	90	
	Recirculation temperature, °C			200
Stack-EL mode	Current density, A/cm^2	0.2	1.1	
	Oxygen inlet flow rate, sccm/cm^2	0	50	
Stack-FC mode	Current density, A/cm^2	0.2	0.6	
	Oxygen inlet flow rate, sccm/cm^2	F_{min}[b]	80	
METH	Pressure, bar	1	30	
	Temperature, °C			290
STN	Pressure level 1, bar	70	170	
	Pressure level 2, bar	10	70	
	Pressure level 3, bar	1	10	
	Pressure level 4, bar			0.05
	Superheating degree 1, °C	50	300	
	Superheating degree 2, °C	1	200	
	Superheating degree 3, °C	1	100	

[a]Dependent variable, calculated by the stack model.
[b]Determined by the maximum oxygen utilization of 30%.

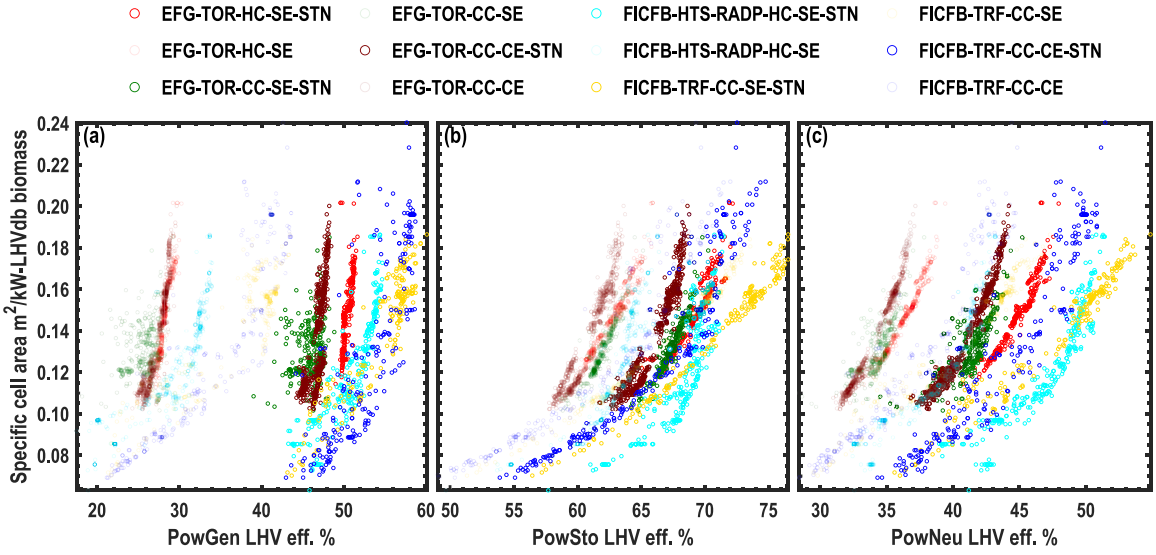

Fig. 6. The design pools of different process options illustrating the trade-off between the efficiency and specific cell area needed per kW-LHVdb biomass. The closed symbols without transparency are the process options with STN, while those with transparency are the process options without STN. The abbreviations of the process options have been explained in Fig. 3. More information for the process options of each type of gasifier is given in the section of additional results in the supplementary materials.

4.2. EFG-TOR-HC-SE-STN

4.2.1. Interaction characteristics

The plant can interact with the electrical grid, the SNG grid and oxygen tanks, as shown in Fig. 7. However, when the optimal designs are derived by minimizing the specific cell area with the suppression of burning syngas, the variations of the interaction scales among different designs become limited for a given biomass feed. The PowGen power export (Fig. 7a) is directly related to the PowGen efficiency, 0.49–0.52 kW/kW-LHVdb; while the PowSto power import can vary within 1.25–1.49 kW/kW-LHVdb. The PowSto SNG production (Fig. 7b) can be within 1.59–1.62 kW-LHVsng/kW-LHVdb, while the PowNeu mode produces less SNG of 0.41–0.48 kW-LHV/kW-LHVdb, due to the syngas-to-electricity-to-SNG conversion. These limited variations are mainly due to that (1) the syngas converted in the stacks is maximized, (2) the variation of stack operating points is accompanied by the change of stack number, and (3) the STN is optimally deployed to maximize heat recovery. When the syngas conversion in the stack is less efficient, meaning more heat is converted from chemical energy, the STN will be automatically enlarged to enhance the heat recovery. This elaboration is further confirmed by Fig. S13 in the supplementary materials, where the optimization was performed by minimizing CAPEX without penalizing the amount of syngas burnt. Thus, the ranges of PowGen and PowSto power capacity, PowSto and PowNeu SNG production capacity extend largely towards small numbers. However, these plant designs in the extended ranges are not interested by the scope of the paper and will not be discussed in detail.

The oxygen balance for all the three modes is shown in Fig. 7c, which is similar for all EFG process options. Both the PowGen and PowNeu modes need net oxygen input, while the PowSto exports oxygen. Since almost all syngas is converted in the stacks in the PowGen and PowSto modes, the oxygen required or generated remains constant. The net oxygen generation of the PowNeu mode increases with efficiency. For the PowNeu mode, the amount of syngas converted to SNG and thus the oxygen generated by the EL stacks increase with the enhanced efficiency. Given the constant oxygen requirement by the gasifier, the net oxygen need of the PowNeu mode reduces with the increased efficiency.

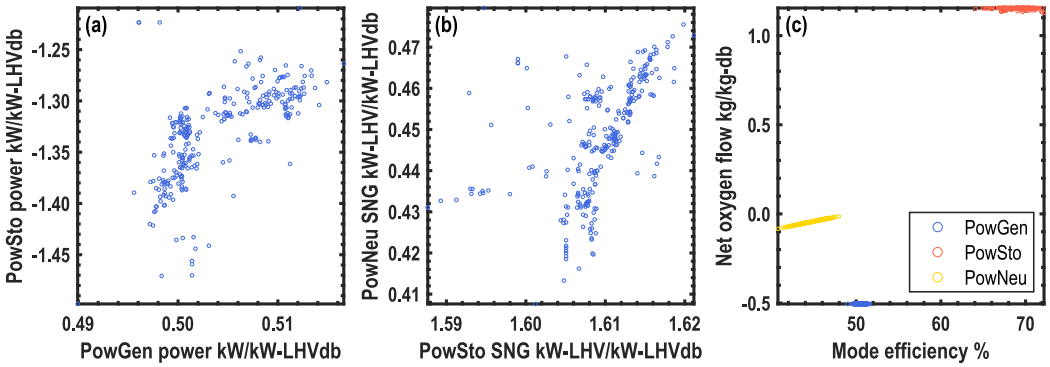

Fig. 7. Characteristics of grid interaction and oxygen management. The positive value stands for "export", while the negative value means "import".

4.2.2. Stack design points

For the PowGen mode in which all stacks work under FC mode, the distributions of the important variables defining the stack design points (Fig. 8) are consistent with our previous observations presented in Ref. [18] with the same efficiency formula (Eq. (1) and (2)) as the objective functions. The current density is the key variable defining the PowGen efficiency and the stack temperature is kept at the maximum allowed level to enhance the stacks' electrochemical performance. The decrease in the current density from 0.35 to 0.2 A/cm^2 can increase the PowGen efficiency from 49 to 52% (Fig. 8a) with the oxygen-side flow rate (Fig. 8b) and utilization factor (Fig. 8c) coordinated for the stack thermal management. Typically, with an increase in current density, the air flow rate will increase from the minimum flow to a larger value, while the utilization factor tends to decrease but remains close to the upper bound (90%). To maximize efficiency, the utilization factor should be kept the highest possible if the stack's thermal management is sufficient. For the PowGen mode, the heat released inside the stacks can be fully managed by the air flow and chemical reactions occurring in the stacks. As a consequence, the air flow rate does not even reach the maximum allowed value (80 sccm/cm^2).

The PowSto mode in which all stacks work under EL mode, the variation trends of the stack design points with efficiency (Fig. 8) are fully consistent with all our past observations in Refs. [18,24–26]. The current density increase from 0.5 to 0.9 A/cm^2 results in an efficiency decrease from 72 to 65%. To cope with the increased heat release in the stack due to the increased overpotential, the oxygen side flow rate thus is increased up to 50 sccm/cm^2 while the utilization factor is reduced to the lower bound (50%). Detailed investigation of such trends of key influencial variables has been given in Refs. [18,24].

4.2.3. Contribution of steam turbine network

The contributions of stacks and STN to the power balance of the three modes are given in Fig. 9. With the minimization of syngas burnt, the contribution of the STN at different modes does not vary significantly among different plant designs presented in the design pool. For the PowGen mode (Fig. 9a), with the target of promoting the use of RSOC stack for syngas conversion, the STN produces much less power than the stacks, since it is used for heat recovery rather than the main generator. With the reduced current density, the stacks generate more power while the STN's contribution is slightly reduced with less heat available for recovery. The STN power contribution remains within 0.21–0.24 kW/kW-LHVdb, around 40% of the total power output (0.49–0.52 kW/kW-LHVdb) with the remaining 0.34–0.38 kW/kW-LHVdb from the RSOC stacks.

For the PowSto mode (Fig. 9b), the STN also produces 0.21–0.24 kW/kW-LHVdb, similar to that of the PowGen mode. This accounts for less than 20% of the total power requirement of the PowSto mode.

For the PowNeu mode (Fig. 9c), the STN (0.21–0.24 kW/kW-LHVdb) contributes slightly less than the stacks under FC mode (0.25–0.27 kW/kW-LHVdb). The power generated by the FC stacks is less than that of the PowGen mode, since a number of RSOC stacks are under EL mode. It can be concluded that for all three modes, the STN generates similar amount of power (0.21–0.24 kW/kW-LHVdb), less than that of the stacks.

If not suppressing the syngas burnt, the contribution of the STN can be largely increased as shown in Fig. S14 in the supplement materials. For the PowGen mode, the power contribution of the STN can be increased to 0.27 kW/kW-LHVdb with the stack contribution reduced to 0.2 kW/kW-LHVdb.

4.2.4. Heat integration

The heat integration related to the SOE technologies has been discussed by the authors in Refs. [9,18,24] for power-to-methane, Refs. [6,7] for biomass-to-fuel, and Ref. [18] for methane-to-power. The key points highlighted were (1) power-to-methane process can potentially be heat self-sufficiency with no use of electrical heating, due to the strongly exothermic methanation reaction at around 300 °C. (2) The methane-to-power process is exothermic and has the potential for heat recovery. As shown in Fig. 10, the process without STN is strongly exothermic for all three modes. Thus, the mature STN has been highlighted as an important means to enhance the overall efficiency. Due to the electricity input of the PowSto mode, its maximum available process heat above 250 °C reaches 0.9 kW/kW-LHVdb, higher than the PowGen mode (0.6 kW/kW-LHVdb) and the PowNeu mode (0.7 kW/kW-LHVdb). The higher value of the PowNeu mode is caused by the additional exergy dissipation from syngas-to-electricity-to-SNG, compared to the syngas-to-electricity of the PowGen mode. With the optimal integration of the 4-pressure-level STN, the available process heat is recovered to a large extent. The operation of the STN of the PowGen and PowNeu modes is similar, while that of the PowSto mode is different to investigate the energy pocket formed by methanation and steam generation.

5. Conclusions

A concept of a three-mode grid balancing plant enabled by biomass gasification and reversible solid-oxide cell stacks is proposed. The plant theoretically can work for power generation, power storage, or even in a power neutral manner. The deployment of such type of plant depends highly on the plant design, grid flexibility needs, and biomass supply chain. To identify potential business cases, a decomposition-based optimization method is presented to systematically consider these factors. However, this paper only investigates the optimal conceptual plant design with a well-established platform, which employs multi-time heat and mass integration platform to consider the three modes simultaneously and multiple objective functions. The target is to create a pool of plant design considering different process configurations. Major conclusions include:

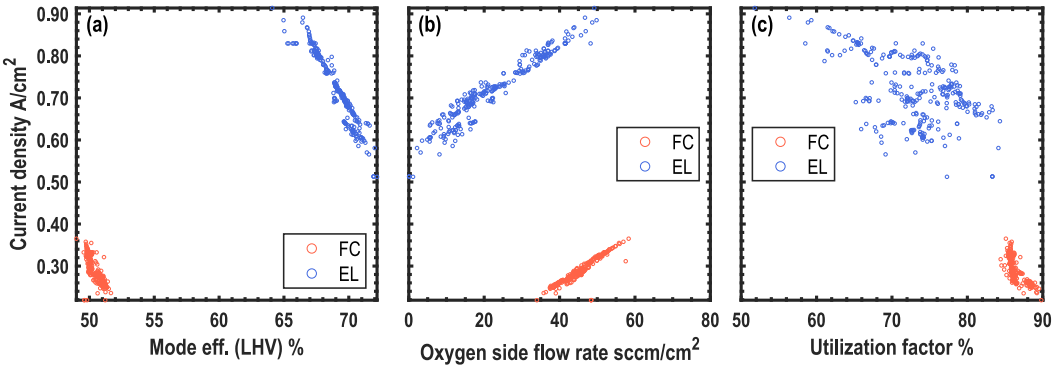

Fig. 8. Stack design points of the optimal plant designs.

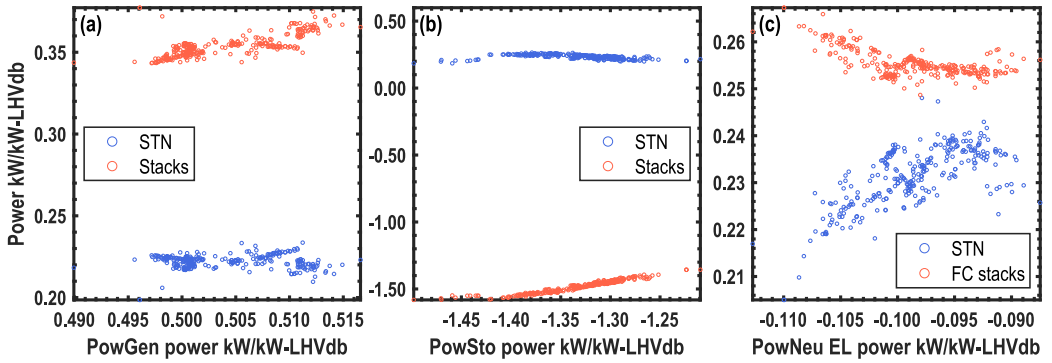

Fig. 9. Contribution of STN to the plant-wise power balance.

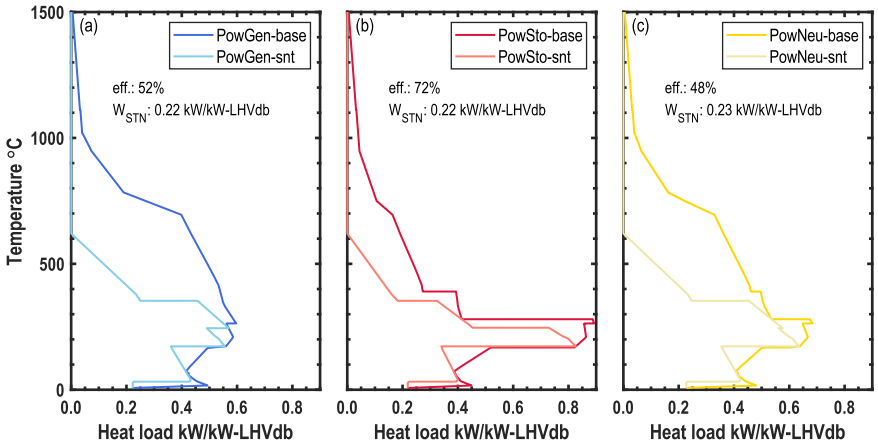

Fig. 10. Integrated composite curves of the design with the highest efficiency. Note that the gasifier is directly heated, thus there is no plateau for heat absorption of the gasifier.

- The increase in efficiency results in an increased cell area for a given biomass feed. There is no big difference (less than 5% points) in efficiency among various process options of the same type of gasifier. The efficiencies reached can be up to 50%–60% (power generation), 72%–76% (power storage) and 47%–55% (power neutral). Those with fluidized bed gasifier can realize higher efficiencies than those with entrained flow gasifier.
- The steam turbine network plays a significant role to enhance the efficiencies of all modes by converting available process heat to electricity. With the promotion of syngas converted electrochemically via penalizing syngas burnt, the Rankine cycle can still generate power of 0.21–0.24 kW/kW-LHVdb, thanks to its optimal deployment. The efficiencies of all three modes can drop by up to 20% points if the steam turbine network is discarded.
- By penalizing the syngas burnt, the optimal designs in the pool obtained has limited variation of grid interactions, particularly for the process options with entrained flow gasifier. The ratio of power between power storage and generation modes can vary within 2.4–3.0, while that of the gas between power storage and power neutral modes varies around 3.5. However, those with fluidized bed gasifier allows for an enlarged ability of grid interactions.
- For all three modes, the overall biomass-to-product processes are highly exothermic. Due to the electricity feed, the PowSto mode results in more process heat (0.9 kW/kW-LHVdb) above 250 °C than the PowGen and PowSto modes (0.6–0.7 kW/kW-LHVdb). Thus, it is a challenge to design a common heat exchanger networks to satisfy the heat transfer of all three modes.

CRediT authorship contribution statement

Ligang Wang: Conceptualization, Data curation, Formal analysis, Methodology, Writing - original draft. **Yumeng Zhang:** Writing - review & editing. **Chengzhou Li:** Writing - review & editing. **Mar Pérez-Fortes:** Validation, Writing - review & editing. **Tzu-En Lin:** Writing - review & editing. **François Maréchal:** Resources, Software, Writing - review & editing. **Jan Van herle:** Funding acquisition, Resources, Writing - review & editing. **Yongping Yang:** Resources, Writing - review & editing.

Declaration of competing interest

The authors declare that they have no known competing financial interests or personal relationships that could have appeared to influence the work reported in this paper.

Acknowledgments

L. Wang, M. Pérez-Fortes and J. Van herle have received funding from the European Union's Horizon 2020 under grant agreement No 826161 (Waste2GridS), 826234 (Waste2Watts), 815284 (BLAZE) and 735692 (CH2P), and support from the Fuel Cells and Hydrogen Joint Undertaking, Hydrogen Europe and Hydrogen Europe research. T.- E. Lin thanks the Young Scholar Fellowship Program by the Ministry of Science and Technology (MOST) in Republic of China, under Grant MOST 108-2636-E-009-012. Y. Zhang, C. Li and Y. Yang thank the financial support by the Science Fund for Creative Research Groups of the National Natural Science Foundation of China (No. 51821004).

L. Wang especially thanks J. Van herle (Group of Energy Materials) and F. Marçchal (Group of Industrial Process and Energy Systems Engineering) for hosting his five-year stay at EPFL (08.2015–07.2020), which firmly enhanced his academic ability. L. Wang also greatly thanks M. Pérez-Fortes for fighting alongside in all EU projects participated during 2016–2020.

Appendix A. Supplementary data

Supplementary material related to this article can be found online at https://doi.org/10.1016/j.apenergy.2020.115987.

References

[1] Directive (eu) 2018/2001 of the european parliament and of the council of 11 december 2018 on the promotion of the use of energy from renewable sources. URL http://data.europa.eu/eli/dir/2018/2001/oj.

[2] eurostat. Energy, transport and environment statistics. Tech. rep., 2019 ed.. 2019, URL https://ec.europa.eu/eurostat/documents/3217494/10165279/KS-DK-19-001-EN-N.pdf/76651a29-b817-eed4-f9f2-92bf692e1ed9.

[3] Arasto A, Chiaramonti D, Kiviluoma J, Waldheim L, Maniatis K, Sipilä K, et al. Bioenergy's role in balancing the electricity grid and providing storage options-an eu perspective. Tech. rep., IEA bioenergy; 2017.

[4] https://www.eea.europa.eu/data-and-maps/indicators/renewable-gross-final-energy-consumption-4/assessment-4 (accessed on 18.06.2020).

[5] Elia Group. Adequacy and flexibility study for Belgium 2020–2030. Tech. rep., Elia Group; 2019, URL https://www.elia.be/-/media/project/elia/elia-site/adequacy-studies/adequacy-studies/20190628_elia_adequacy_{and}_flexibility_study_2020_2030_nl_archive.pdf.

[6] Zhang H, Wang L, Pérez-Fortes M, Maréchal F, Desideri U, et al. Techno-economic optimization of biomass-to-methanol with solid-oxide electrolyzer. Appl Energy 2020;258:114071.

[7] Zhang H, Wang L, Maréchal F, Desideri U, et al. Techno-economic evaluation of biomass-to-fuels with solid-oxide electrolyzer. Appl Energy 2020;270:115113.

[8] Zhang H, Wang L, Maréchal F, Desideri U, et al. Techno-economic comparison of green ammonia production processes. Appl Energy 2020;259:114135.

[9] Wang L, Chen M, Küngas R, Lin T-E, Diethelm S, Maréchal F, et al. Power-to-fuels via solid-oxide electrolyzer: Operating window and techno-economics. Renew Sustain Energy Rev 2019;110:174–87.

[10] Jensen SH, Graves C, Mogensen M, Wendel C, Braun R, Hughes G, Gao Z, Barnett S. Large-scale electricity storage utilizing reversible solid oxide cells combined with underground storage of CO2 and CH4. Energy Environ Sci 2015;8(8):2471–9.

[11] Mottaghizadeh P, Santhanam S, Heddrich MP, Friedrich KA, Rinaldi F. Process modeling of a reversible solid oxide cell (r-SOC) energy storage system utilizing commercially available SOC reactor. Energy Convers Manage 2017;142:477–93.

[12] Santhanam S, Heddrich MP, Riedel M, Friedrich KA. Theoretical and experimental study of reversible solid oxide cell (r-soc) systems for energy storage. Energy 2017;141:202–14.

[13] Reznicek EP, Braun RJ. Reversible solid oxide cell systems for integration with natural gas pipeline and carbon capture infrastructure for grid energy management. Appl Energy 2020;259:114118.

[14] Sigurjonsson HÆ, Clausen LR. Solution for the future smart energy system: A polygeneration plant based on reversible solid oxide cells and biomass gasification producing either electrofuel or power. Appl Energy 2018;216:323–37.

[15] Butera G, Jensen SH, Gadsbøll RØ, Ahrenfeldt J, Clausen LR. Flexible biomass conversion to methanol integrating solid oxide cells and twostage gasifier. Fuel 2020;271:117654.

[16] Perna A, Minutillo M, Lavadera AL, Jannelli E. Combining plasma gasification and solid oxide cell technologies in advanced power plants for waste to energy and electric energy storage applications. Waste Manage 2018;73:424–38.

[17] De Buck P. Energy transition in europe: the case for gas and gas infrastructure. In *United Nations conference on trade and development, 8th global commodities forum, 23-24 2018*, Geneva, 2018.

[18] Wang L, Zhang Y, Pérez-Fortes M, Aubin P, Lin T-E, Yang Y, Maréchal F, et al. Reversible solid-oxide cell stack based power-to-x-to-power systems: Comparison of thermodynamic performance. Appl Energy 2020;275:115330.

[19] Peduzzi E. Biomass to liquids: Thermo-economic analysis and multi-objective optimisation (Ph.D. thesis), École Polytechnique Fédérale de Lausanne; 2015.

[20] Olsen KP, Zong Y, You S, Bindner H, Koivisto M, Gea-Bermúdez J. Multi-timescale data-driven method identifying flexibility requirements for scenarios with high penetration of renewables. Appl Energy 2020;264:114702.

[21] Biomass Energy Europe: http://www.eu-bee.eu/.

[22] S2Biom Delivery of sustainable supply of non-food biomass to support a resource-efficient Bioeconomy in Europe: https://www.s2biom.eu/en/.

[23] Biomass Future: https://ec.europa.eu/energy/intelligent/projects/en/projects/biomass-futures.

[24] Wang L, Pérez-Fortes M, Madi H, Diethelm S, Maréchal F, et al. Optimal design of solid-oxide electrolyzer based power-to-methane systems: A comprehensive comparison between steam electrolysis and co-electrolysis. Appl Energy 2018;211:1060–79.

[25] Wang L, Düll J, Maréchal F, Van herle J. Trade-off designs and comparative exergy evaluation of solid-oxide electrolyzer based power-to-methane plants. Int J Hydrogen Energy 2019;44(19):9529–43. http://dx.doi.org/10.1016/j.ijhydene.2018.11.151, URL http://www.sciencedirect.com/science/article/pii/S0360319918337832 special Issue on Power To Gas and Hydrogen applications to energy systems at different scales - Building, District and National level.

[26] Wang L, Rao M, Diethelm S, Lin T-E, Zhang H, Hagen A, Maréchal F, et al. Power-to-methane via co-electrolysis of h2o and co2: The effects of pressurized operation and internal methanation. Appl Energy 2019;250:1432–45.

[27] Kavvadias K, Hidalgo Gonzalez I, Zucker A, Quoilin S. Integrated modelling of future eu power and heat systems-the dispa-set V2. 2 open-source model. Tech. rep, European Commission; 2018.

[28] Puigjaner L. Syngas from waste: Emerging technologies. Springer; 2011.

[29] Laínez JM, Pérez-Fortes M, Bojarski AD, Puigjaner L. Raw materials supply. In: Syngas from waste. Springer; 2011, p. 23–54.

[30] Pérez-Fortes M, Laínez-Aguirre JM, Bojarski AD, Puigjaner L. Optimization of pre-treatment selection for the use of woody waste in co-combustion plants. Chem Eng Res Des 2014;92(8):1539–62.

[31] Kantor I, Robineau J-L, Butun H, Marechal F. A mixed-integer linear programming formulation for optimizing multi-scale material and energy integration. Front Energy Res 2020;8(ARTICLE):49.

[32] Goodwin DG, Speth RL, Moffat HK, Weber BW. Cantera: An object-oriented software toolkit for chemical kinetics, thermodynamics, and transport processes. 2018, http://dx.doi.org/10.5281/zenodo.1174508, https://www.cantera.org, version 2.4.0.

[33] Turton R, Bailie RC, Whiting WB, Shaeiwitz JA. Analysis, synthesis and design of chemical processes. Pearson Education; 2008.

[34] Kermani M, Wallerand AS, Kantor ID, Maréchal F. Generic superstructure synthesis of organic rankine cycles for waste heat recovery in industrial processes. Appl Energy 2018;212:1203–25.

[35] Wallerand AS, Kermani M, Kantor I, Maréchal F. Optimal heat pump integration in industrial processes. Appl Energy 2018;219:68–92.